View Online

PAPER

NJC
www.rsc.org/njc

Self-assembly and properties of phthalocyanine and polyelectrolytes onto melamine resin particles

Xia Tao,†*[a] Junbai Li,[b] Jürgen Hartmann[a] and Helmuth Möhwald[a]

[a] *Max-Planck Institute of Colloids and Interfaces, Am Mühlenberg 2, 14424 Potsdam, Germany. E-mail: taoxia@yahoo.com*
[b] *International Joint Lab, Institute of Chemistry, Chinese Academy of Sciences, Beijing, 100080 P.R. China*

Received (in Toulouse) 30th June 2004, Accepted 17th September 2004
First published as an Advance Article on the web 17th November 2004

Hollow capsules have been prepared by electrostatic layer-by-layer self-assembly of tetrasulfophthalocyanine iron [Fe(PcS$_4$)] in alternation with poly(diallyldimethylammonium chloride) (PDDA) onto the precursor shells with well-defined internal volumes. The resultant linear deposition process was monitored by UV/Vis absorption spectra, microelectrophoresis, and scanning force microscopy (SFM). The formation of intact spherical capsules was verified by confocal laser scanning microscopy and SFM. A mean density of *ca.* 3 [Fe(PcS$_4$)] molecules per nm^2 and a wall thickness of 2.7 ± 0.2 nm for each PDDA/[Fe(PcS$_4$)] bilayer were obtained. The characteristic maximum absorption of [Fe(PcS$_4$)] in the coating suggests that [Fe(PcS$_4$)] exists mainly in the form of an aquo complex [HOFe^{III}(PcS$_4$)]. The fabricated hollow capsules display a high stability in response to light irradiation and high temperature.

Introduction

In recent years, hollow capsules have attracted considerable attention due to their scientific and technological importance in many fields, for example, as well-defined internal volumes for the encapsulation of active ingredients, the preparation of nanostructured materials, for drug delivery, heterogeneous catalysis, and as artificial light-harvesting antenna for solar energy conversion.[1,2] However, deformation and rupture of hollow capsules under adverse conditions (*e.g.*, light irradiation and high temperature) may limit their general application. While the stability of hollow capsules can be modified[3,4] by incorporating inorganic particles into the shells, changing the structure of the shells or depositing additional layers, it is still desirable to construct different composite capsules with high optical and thermal stability as required for specific applications.

Phthalocyanines may form a new class of biomimetic complexes with promising properties for potential use in photodynamic therapy and in optical or photoelectrochemical applications.[5–7] Tetrasulfophthalocyanine iron [Fe(PcS$_4$)] with symmetrically charged structures, as a representative of the phthalocyanine family, has been employed as an efficient (photo)catalyst in the selective oxidation and treatment of persistent organic pollutants in water.[8,9] [Fe(PcS$_4$)] possesses good photostability, thermal stability, super selectivity, and inertness to molecular oxygen, thereby making [Fe(PcS$_4$)] a favorable system capable of operating in harsh biological and artificial environments.

The layer-by-layer (LbL) self-assembly technique driven through electrostatic interactions has been widely utilized to create novel nano- and microcapsules.[10,11] The typical hollow polyelectrolyte capsules produced so far can be formed by repetitive alternating adsorption of poly(sodium 4-styrenesulfonate) (PSS) and poly(allylamine hydrochloride) (PAH) on colloidal templates, followed by removal of the cores. In this work, we fabricated a novel capsule by alternately assembling poly(diallyldimethylammonium chloride) (PDDA) and [Fe(PcS$_4$)] on the precursor shells of (PSS/PAH)$_3$/PSS. The stepwise growth of multilayer films on spherical surfaces was monitored by UV/Vis spectroscopy and microelectrophoresis. The characteristic absorption bands of [Fe(PcS$_4$)] in aqueous solutions and in solutions of the capsules were analyzed in great detail to reveal the state of the [Fe(PcS$_4$)] molecules in the different microenvironments. The optical and thermal stability of the capsules was elucidated by observing UV/Vis absorption spectral changes and by confocal laser scanning microscopy images under different conditions: prior to and after light irradiation as well as after heating. It was found that the fabricated hollow capsules possess highly optical stability and are thermally extremely stable.

Experimental

Materials

PSS (M_w ~70 000), PAH (M_w ~70 000), PDDA (20 wt % in water, M_w ~200 000–350 000) and [Fe(PcS$_4$)] were purchased from Aldrich Chemical Co. Weakly crosslinked melamine formaldehyde particles (MF, 5 μm) and polystyrene particles (PS, 488 nm), used as the colloidal templates, were purchased from Microparticles GmbH, Berlin, Germany. All chemicals were used as received. For reference, the chemical structures of [Fe(PcS$_4$)], PSS, PAH, and PDDA are shown in Fig. 1.

A solution of [Fe(PcS$_4$)] with a concentration of 1.7×10^{-4} M in 0.01 M phosphate buffer solution of pH 7.4 was prepared as stock solution. This solution is stable at room temperature for several months. Solutions of PSS (1 mg ml^{-1}), PAH (1 mg ml^{-1}) and PDDA (1 mg ml^{-1}) with 0.5 M NaCl were prepared for all experiments. Ultrapure water (Millipore) with a resistance higher than 18 MΩ cm was used throughout the study.

---

† Present address: Faculty of Pharmacy and Pharmaceutical Sciences, 3118 Pharmacy Center, University of Alberta, Edmonton, AB T6G 2N8, Canada.

DOI: 10.1039/b409993a

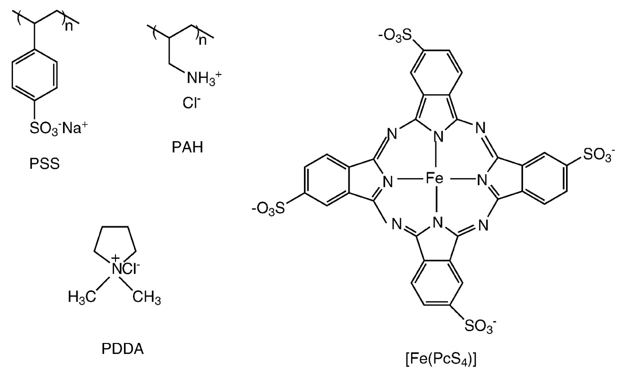

Fig. 1 Chemical structures of poly(sodium 4-styrenesulfonate) (PSS), poly(allylamine hydrochloride) (PAH), poly(diallyldimethylammonium chloride) (PDDA) and the biomimetic complex tetrasulfophthalocyanine iron [Fe(PcS_4)] used in this study.

Capsule and multilayer preparation

The typical hollow capsules composed of PSS and PAH were fabricated by repetitive alternating adsorption of PSS and PAH on the colloidal templates (MF), followed by removal of the cores.[3b,12] After formation of hollow capsules of $(PSS/PAH)_3/PSS$, PDDA and [Fe(PcS_4)] were alternately added to the as-prepared capsule solutions and left to adsorb for 30 min each. The excess PDDA or [Fe(PcS_4)] was removed by three repeated centrifugation (2500 g, 5 min)/washing/redispersion cycles with dilute aqueous NaCl in each deposition step. Subsequent layers were deposited in the same manner as described above up to the desired number of deposition cycles. All adsorption procedures were carried out at ambient temperature.

Light source

A 150 W super-quiet xenon lamp (Hamamatsu, Japan) was positioned inside the E7536 lamp housing with an automatic cooling fan (Hamamatsu, Japan). One side of the lamp housing has a window with an area of *ca.* 3 × 3 cm^2. A cutoff filter able to completely block wavelengths shorter than 400 nm was placed on the small window. The center-to-center distance between the reaction vessel and the light source was 6 cm.

Characterization methods

Absorption spectra of hollow capsules were measured in Millipore water on a Varian Cary 4E UV/Vis spectrophotometer.

Multilayer growth of the assembled hollow capsule walls on MF particles was followed by measuring the microelectrophoretic mobility of the coated particles using a Malvern Zetasizer 4, taking the average of six measurements at the stationary level. The mobility (u) was converted into the zeta potential (ζ) by using the Smoluchowski relation ($\zeta = u\eta/\varepsilon$), in which η and ε are the viscosity and permittivity of the solution, respectively.

Confocal laser scanning microscopy (CLSM) images were taken with a Leica TCS NT microscope (Germany) equipped with a 100× oil immersion objective.

Scanning force microscopy (SFM) images were recorded using a Digital Instruments Nanoscope IIIa in tapping mode. Samples were prepared by applying a drop of the capsule solution onto a freshly cleaved mica substrate. After the capsules were allowed to settle, the substrate was extensively rinsed in Millipore water and then dried under a gentle stream of nitrogen.

Transmission electron microscopy (TEM) measurements were performed on a Leo 912 Omega microscope operated at 120 kV.

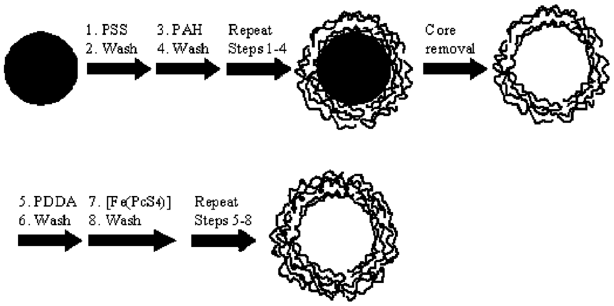

Scheme 1 Schematic illustration for the preparation of hollow PDDA/[Fe(PcS_4)] multilayer capsules.

Results and discussion

Scheme 1 shows the general procedure of LbL self-assembly of PDDA/[Fe(PcS_4)] onto the $(PSS/PAH)_3/PSS$ shells templated on MF latex particles. [Fe(PcS_4)] possesses a large planar porphyrin-like macrocycle with four sulfonato groups. In neutral buffer solution [Fe(PcS_4)] exhibits a complete degree of ionization and is capable of strongly interacting with the ammonium groups of the polyelectrolyte PDDA by electrostatic interactions.[13] The partial degree of ionization of [Fe(PcS_4)] in strongly acidic media at pH 1 leads to weak interactions between [Fe(PcS_4)] and PDDA. This has been deduced from the fact that obvious desorption of [Fe(PcS_4)] from the capsule walls occurs upon exposing PDDA/[Fe(PcS_4)] multilayer-coated MF particles to 0.1 M HCl for dissolution of the core templates. Therefore, in order to avoid desorption of [Fe(PcS_4)] from the shells during the core removal procedure, we first build up $(PSS/PAH)_3/PSS$ shells as a precursor, followed by alternating adsorption of [Fe(PcS_4)] and PDDA until the desired number of multilayers is obtained (see experimental for details).

The assembled capsule solutions exhibit the characteristic blue color of [Fe(PcS_4)]. The absorption spectra of multilayer assemblies and the changes of the peak absorption with the number of deposition cycles can be easily monitored by UV/Vis spectroscopy. Fig. 2 shows a typical series of absorption spectra for the fabrication of the PDDA/[Fe(PcS_4)] multilayer hollow capsules. The maximum absorption peaks of [Fe(PcS_4)]

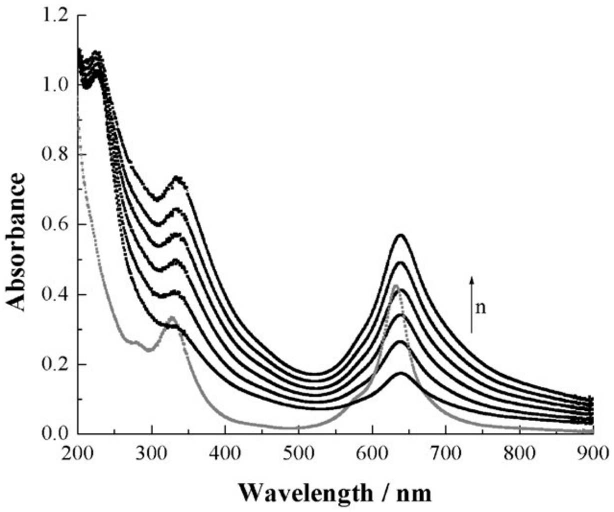

Fig. 2 UV/Vis absorption spectra of $\{PDDA/[Fe(PcS_4)]\}_n$ (n = 1–6) alternating assemblies of hollow capsules of $(PSS/PAH)_3/PSS$ obtained by removal of the 5 μm MF cores with 0.1 M HCl, measured after [Fe(PcS_4)] adsorption at each deposition cycle. The resulting capsules were dispersed in Millipore water at the given volume for measurements. The dotted curve shows the absorption of [Fe(PcS_4)] dissolved in 0.01 M phosphate buffer solution of pH 7.4.

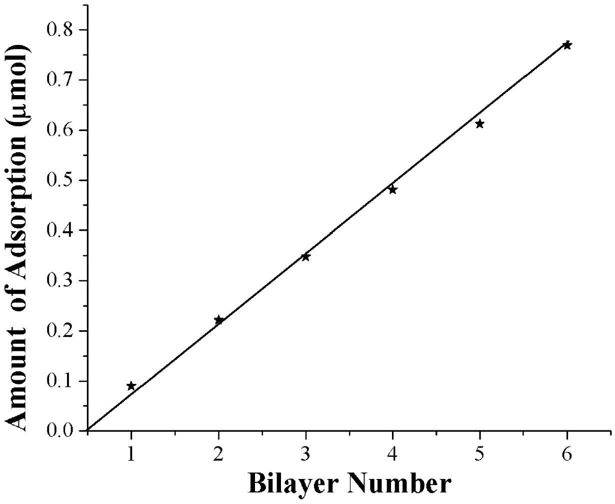

Fig. 3 Amount of deposited [Fe(PcS$_4$)] on the shells as a function of the number of {PDDA/[Fe(PcS$_4$)]}$_n$ bilayers (n = 1–6). The amount of [Fe(PcS$_4$)] bound to the capsule walls per PDDA/[Fe(PcS$_4$)] bilayer can be estimated by the difference between the initial concentration of [Fe(PcS$_4$)] added and the entirely nonadsorbed amount of [Fe(PcS$_4$)] obtained from the supernatant liquids after three repeated centrifugation/washing/redispersion cycles, with a molar extinction coefficient of 5.6×10^4 M^{-1} cm^{-1} for [Fe(PcS$_4$)] in aqueous solution at 632 nm.

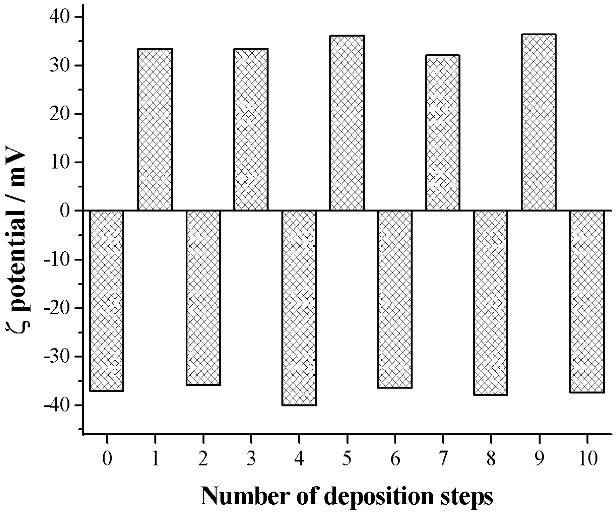

Fig. 4 ζ potential of PAH/PSS/PDDA/[Fe(PcS$_4$)] multilayers on 488 nm PS latex particles as a function of the number of deposition steps. The odd layer numbers correspond to PAH (n = 1, 3) and PDDA (n = 5, 7, 9) deposition. The even layer numbers correspond to PSS (n = 2, 4) and Fe(PcS$_4$) (n = 6, 8, 10) adsorption. The uncovered PS latex particles exhibit a ζ potential of *ca.* −37 mV.

at 334 nm (Soret band) and at 636 nm (Q band) are observed to increase almost in proportion with the number of [Fe(PcS$_4$)] layers nominally deposited. The linear increase of absorbance with the number of deposition cycles indicates successful deposition at each step as well as reproducibility and controllability of the whole deposition process.

In aqueous solution, the maximum absorption of [Fe(PcS$_4$)] (the dotted spectrum in Fig. 2) in the visible spectral range is located at 632 nm, which is a slight blue-shift of 4 nm compared with that of the PDDA/[Fe(PcS$_4$)] multilayer capsule solutions. Interestingly, the maximum absorption wavelengths of [Fe(PcS$_4$)] from the supernatant liquids collected by repeated rinsing with water and centrifugation in each deposition step or from the supernatant of the capsule solutions upon exposing PDDA/[Fe(PcS$_4$)] multilayer-coated MF particles to 0.1 M HCl are again seen at 632 nm, which implies the transformation of existing forms of [Fe(PcS$_4$)] in a different microenvironment. The absorption band of [Fe(PcS$_4$)] at 636 nm as observed in the capsule solutions can be attributed to the aquo complex [HOFe^{III}(PcS$_4$)], which is proposed to be the catalytically active complex for the degradation and mineralization of organic pollutants under visible light irradiation.[9,14]

Fig. 3 displays the amount of [Fe(PcS$_4$)] deposited in the capsule walls *versus* the number of bilayers. It is seen that the amount of [Fe(PcS$_4$)] deposited increases linearly with increasing number of adsorption cycles. From the slope of the line i.e. 0.128 μmol per bilayer, and a surface area estimation of the three-dimensional distribution of microparticles with a capsule diameter of 5.0×10^{-4} cm, a particle density of 1.51 g cm^{-3}, a particle content of 10 wt % and a sampled suspension volume of 300 μl, a mean density of *ca.* 3 [Fe(PcS$_4$)] molecules per nm^2 is estimated. This is a rather large amount in view of the fact that the molecular cross section of [Fe(PcS$_4$)] is about 1 nm^2 and indicates that the macrocycles of [Fe(PcS$_4$)] are likely to lie perpendicular to the diameter of the capsules, thus with a projected molecular area significantly lower than 1 nm^2. This explanation is also in agreement with the measured film thickness per PDDA/[Fe(PcS$_4$)] bilayer (see below). Actually, such a way of incorporating [Fe(PcS$_4$)] within a hollow capsule allows nucleophilic oxidants to be easily added to the electrophilic iron center of [Fe(PcS$_4$)] in the axial direction, thus leading to an enhancement of the catalytic activity of [Fe(PcS$_4$)].[9,13]

Microelectrophoresis measurements were utilized to follow the number of layers on MF latex particles. Fig. 4 shows the stepwise assembly of PSS, PAH, PDDA and [Fe(PcS$_4$)] on PS particles. An initial value of *ca.* −37 mV corresponds to uncovered PS latex particles. Subsequent alternating ζ potentials are an excellent indicator of multilayer film growth.[15,16] ζ potential values from layer 1 to layer 4 correspond to alternating deposition of PSS and PAH, while ζ potential values from layer 5 to layer 10 follow the subsequent alternating deposition of PDDA and [Fe(PcS$_4$)]. It is worth noting that [Fe(PcS$_4$)] as the outmost layer yields a ζ potential of *ca.* −37 mV, which indicates that [Fe(PcS$_4$)] with four negative charges is effective in reversing the sign of the surface charge when deposited alternately with PDDA. On the whole, the alternating ζ potentials observed with each coating step strongly

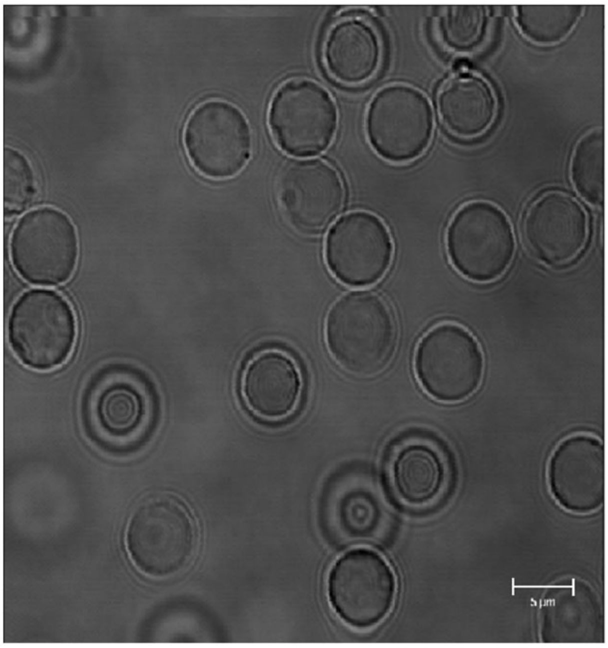

Fig. 5 CLSM transmission images of hollow capsules of (PSS/PAH)$_3$/PSS/[PDDA/[Fe(PcS$_4$)]]$_4$ templated on MF latex particles. The scale bar corresponds to 5 μm.

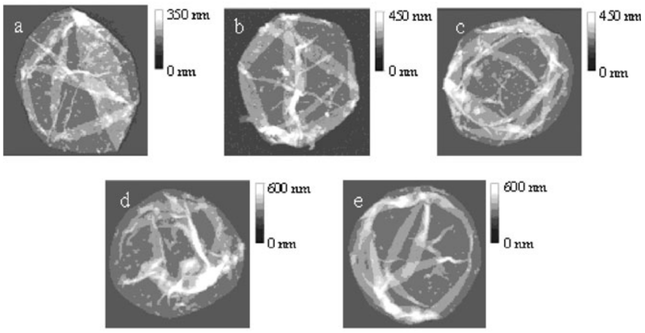

Fig. 6 SFM images of capsules of $(PSS/PAH)_3/PSS/\{PDDA/[Fe(PcS_4)]\}_n$ templated onto 5 μm MF latex particles. (a) $n = 1$, (b) $n = 2$, (c) $n = 3$, (d) $n = 4$, (e) $n = 5$.

suggest the multilayer growth of the fabricated capsules and also support the UV/Vis measurements shown in Fig. 2.

Direct visualization of hollow capsules composed of $(PSS/PAH)_3/PSS/\{PDDA/[Fe(PcS_4)]\}_4$ was provided by CLSM measurements, as shown in Fig. 5. The assembled hollow capsules remain intact and spherical after repeated alternating adsorption of PDDA and $[Fe(PcS_4)]$ on the $(PSS/PAH)_3/PSS$ shells. This indicates that any additional force arising from adsorption of $[Fe(PcS_4)]$ on the capsule surfaces is minor, being incapable of leading to deformation and destruction of the whole capsule. Recently, we fabricated different hollow capsules with tetrasulfophthalocyanine aluminium $[Al(PcS_4)]$, Congo red (biphenylylenediazo-bis-1-naphthylamine-4-sulfonic acid disodium salt) or Orange II [4-(2-hydroxy-1-naphthylazo)benzenesulfonic acid sodium salt] as a component of the capsule walls instead of $[Fe(PcS_4)]$ and found that the hollow capsules composed of $[Al(PcS_4)]$ or Congo red remained as intact spherical replicas of the template particles, but that deposition of Orange II resulted in destruction of the spherical shape.[16] In regards to their different molecular structures, it is reasonable to consider that species with a symmetrical charge distribution facilitate construction of stable hollow capsules.

Fig. 6 shows SFM images of capsules with different numbers of $PDDA/[Fe(PcS_4)]$ bilayers assembled on the $(PSS/PAH)_3/PSS$ shells. It is seen that the three-dimensional composite shells are continuous films in which a number of folds and creases arising from evaporation of the aqueous content upon air drying are discerned. In order to obtain quantitative evidence for the formation of $PDDA/[Fe(PcS_4)]$ multilayers on the $(PSS/PAH)_3/PSS$ shells, the wall thickness of these capsules was determined from the minimum height of the air-dried hollow capsules. This value corresponds to twice the capsule wall thickness. Fig. 7 displays the thickness of the capsule walls related to different numbers of deposition cycles. An increase of 2.7 ± 0.2 nm in the thickness of the shells was observed for each $PDDA/[Fe(PcS_4)]$ layer, a value comparable to those found for other multilayers.[17] The linear growth of the wall thickness with increasing number of deposition cycles is in good agreement with the results from absorption spectra (Fig. 2) and microelectrophoresis measurements (Fig. 4).

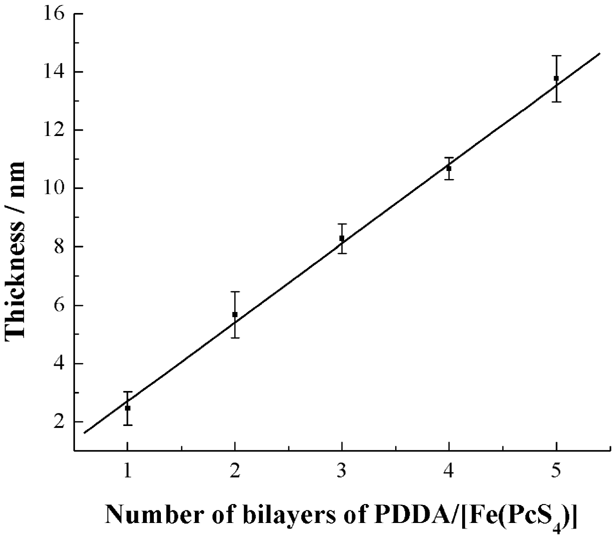

Fig. 7 Thickness of capsule walls of $(PSS/PAH)_3/PSS/[PDDA/\{Fe(PcS_4)]\}_n$ (n = 1–5) onto 5 μm MF latex particles with neutral wash (pH 7).

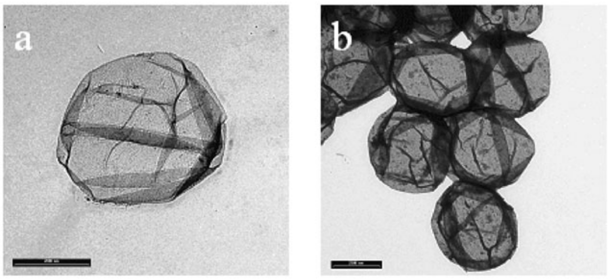

Fig. 8 TEM images of air-dried hollow capsules of $(PSS/PAH)_3/PSS/\{PDDA/[Fe(PcS_4)]\}_n$ templated onto 5 μm MF latex particles. (a) $n = 2$, (b) $n = 5$.

The hollow capsules produced with different $PDDA/[Fe(PcS_4)]$ layers were further characterized using TEM (Fig. 8). Evidently, the wall thickness of the composite $(PSS/PAH)_3/PSS/\{PDDA/[Fe(PcS_4)]\}_5$ capsules is larger than that of the composite $(PSS/PAH)_3/PSS/\{PDDA/[Fe(PcS_4)]\}_2$ capsules, which provides further evidence for growth of the walls with increasing number of $PDDA/[Fe(PcS_4)]$ deposition cycles.

The optical and thermal stability of the capsules was elucidated by observing UV/Vis absorption spectral changes and confocal laser scanning microscopy (CLSM) images under different conditions, prior to and after light irradiation as well as heating. An aqueous capsule solution composed of $(PSS/PAH)_3/PSS/\{PDDA/[Fe(PcS_4)]\}_3$ was irradiated for 3 h with a 150 W super-quiet xenon lamp (light filter $<$400 nm). No spectra changes are observed prior to and after irradiation and CLSM images show that the hollow capsules remain intact and spherical even after irradiation. In addition, upon heating the $PDDA/[Fe(PcS_4)]$ hollow capsule solutions at 185 °C for 12 h, all the hollow capsules with a diameter of *ca.* 5 μm are shape-persistent and no UV/Vis absorption spectra changes occur throughout the entire heating process. All these observations indicate that the fabricated hollow capsules are very stable over a wide Vis/near IR light irradiation region and also thermally highly stable.

Conclusion

We have constructed a novel capsule composed of tetrasulfophthalocyanine iron $[Fe(PcS_4)]$ and polyelectrolytes *via* the electrostatic layer-by-layer (LbL) self-assembly technique. The layers grow linearly, yielding an average film thickness of *ca.* 2.7 nm per bilayer. The resulting hollow capsules display high optical and thermal stability. The LbL engineering of multilayer capsules based on $[Fe(PcS_4)]$ and polyelectrolytes can be considered as an efficient immobilized (photo)catalyst for selective oxidation and degradation. A mean density of *ca.* 3 $[Fe(PcS_4)]$ molecules per nm^2 and a wall thickness of 2.7 ± 0.2 nm for each $PDDA/[Fe(PcS_4)]$ bilayer were obtained.

Acknowledgements

This work was supported financially by the international joint laboratory between the German Max-Planck-Society and

Chinese Academy of Sciences. The authors thank Anne Heilig for experimental assistance with the SFM measurements and Heidi Zastrow for help with the electrophoresis measurements.

References

1 (*a*) A. D. Dinsmore, M. F. Hsu, M. G. Nikolaides, M. Marquez, A. R. Bausch and D. A. Weitz, *Science*, 2002, **298**, 1006–1009; (*b*) Y. Lin, H. Skaff, T. Emrick, A. D. Dinsmore and T. P. Russell, *Science*, 2003, **299**, 226–229; (*c*) T. Joki, M. Machluf, A. Atala, J. Zhu, N. T. Seyfried, I. F. Dunn, T. Abe, R. S. Carroll and P. M. Black, *Nature Biotechnol.*, 2001, **19**, 35–39.

2 (*a*) E. Donath, G. B. Sukhorukov, F. Caruso, S. A. Davis and H. Möhwald, *Angew. Chem.*, 1998, **110**, 2324–2327; (*b*) E. Donath, G. B. Sukhorukov, F. Caruso, S. A. Davis and H. Möhwald, *Angew. Chem., Int. Ed.*, 1998, **37**, 2201–2205.

3 (*a*) Z. Dai and H. Möhwald, *Chem.-Eur. J.*, 2002, **8**, 4751–4755; (*b*) Z. Dai, L. Dähne, H. Möhwald and B. Tiersch, *Angew. Chem.*, 2002, **114**, 4191–4194; (*c*) Z. Dai, L. Dähne, H. Möhwald and B. Tiersch, *Angew. Chem., Int. Ed.*, 2002, **41**, 4019–4022.

4 L. Ge, H. Möhwald and J. Li, *Biochem. Biophys. Res. Commun.*, 2003, **303**, 653–659.

5 H. Ali, R. Langlois, J. R. Wagner, N. Brasseur, B. Paquette and J. E. Lier, *Photochem. Photobiol.*, 1988, **47**, 713–717.

6 N. B. McKeown, *Phthalocyanine Materials: Synthesis, Structure and Function*, Cambridge University Press, Cambridge, UK, 1998.

7 H. Kim, I. Rosenthal, L. Kirschenbaum and P Riesz, *Free Radical Biol. Med.*, 1992, **13**, 231–238.

8 (*a*) A. Sorokin, J.-L. Séris and B. Meunier, *Science*, 1995, **268**, 1163–1165; (*b*) B. Meunier and A. Sorokin, *Acc. Chem. Res.*, 1997, **30**, 470–476; (*c*) L. Wei, X. Chen, H. Yang and J. Xu, *Anal. Sci.*, 2002, **18**, 585–589.

9 X. Tao, W. Ma, T. Zhang and J. Zhao, *Chem.-Eur. J.*, 2002 **8**, 1321–1326.

10 G. Decher, *Science*, 1997, **277**, 1232–1237.

11 (*a*) M. Matsumoto, D. Miyazaki, M. Tanaka, R. Azumi, E. Manda, Y. Kondo, N. Yoshino and H. Tachibana, *J. Am. Chem. Soc.*, 1998, **120**, 1479–1484; (*b*) S. Leporatti, C. Gao, A. Voigt, E. Donath and H. Möhwald, *Eur. Phys. J. E*, 2001, **5**, 13–20.

12 (*a*) X. Tao, J. Li and H. Möhwald, *Chem.-Eur. J.*, 2004, **10**, 3397–3403; (*b*) X. P. Qiu, S. Leporatti, E. Donath and H. Möhwald, *Langmuir*, 2001, **17**, 5375–5380.

13 X. Tao, W. Ma, J. Li, Y. Huang, J. Zhao and J. C. Yu, *Chem. Commun.*, 2003, 80–81.

14 A. Hadasch, A. Sorokin, A. Rabion and B. Meunier, *New J. Chem.*, 1998, 45–51.

15 (*a*) C. Gao, E. Donath, H. Möhwald and J. Shen, *Angew. Chem.*, 2002, **114**, 3943–3947; (*b*) C. Gao, E. Donath, H. Möhwald and J. Shen, *Angew. Chem., Int. Ed.*, 2002, **41**, 3789–3793.

16 C. Gao, H. Möhwald and J. Shen, *Adv. Mater.*, 2003, **15**, 930–933.

17 (*a*) J. He, S. Bian, L. Li, J. Kumar and S. K. Tripathy, *J. Phys. Chem.*, 2000, **104**, 10513–10521; (*b*) S. Leporatti, A. Voigt, R. Mitlöhner, G. Sukhorukov, E. Donath and H. Möhwald, *Langmuir*, 2000, **16**, 4059–4063.